Original
Received February 7, 2002
Accepted for Publication June 19, 2002

Effect of Zn Addition to Sn-3Ag-5Bi Solder on Joint Strength and Joint Interface

Yuunosuke NAKAHARA*, Ryuuji NINOMIYA*, Michihiro TAGAMI**,
Mikio SUGAI** and Shinichi NAKATA**

*Corporate R&D Center, Mitsui Mining & Smelting Co., LTD., 1333-2, Haraichi, Ageo-shi, Saitama 362-0021 Japan
E-mail : y_nakahara@mitsui-kinzoku.co.jp, r_ninomiya@mitsui-kinzoku.co.jp
**Faculty of Engineering and Resource Science, Akita University, Japan
E-mail : tagami@ipc.akita-u.ac.jp, sugai@ipc.akita-u.ac.jp, snakata@ipc.akita-u.ac.jp

The mechanical properties and the joint strength of Sn-Ag-Bi solders as replacement solders for Sn-Pb eutectic solder were investigated. The joint strength between Cu sheets and solder decreases when more than 5 mass% Bi is added to Sn-Ag system solders after annealing. Zn addition to Sn-3Ag-5Bi solder is carried out in order to improve the joint strength. The effect of Zn addition to Sn-3Ag-5Bi solder on the joint strength and the joint interface structure was investigated. Zn addition to Sn-3Ag-5Bi solder changes the joint interface structure from solder/Cu-Sn intermetallic compounds/Cu to solder/Cu-Zn intermetallic compound/Cu-Sn intermetallic compound/Cu. Cu-Zn intermetallic compound acts as a barrier layer for inhibiting the growth of Cu-Sn reaction layer. Therefore, the growth of reaction layer and decrease of joint strength are inhibited by Zn addition after annealing.

Key Words : Lead-free solder, Zn addition, Joint strength, Reaction layer, Joint interface structure.

1. Introduction

Sn-Pb eutectic solder has been widely used in the electronics industry because of its low melting temperature, low cost, good wettability, high ductility and good joint strength. However, due to increasing environmental and health concerns regarding the toxicity of lead, a lead-free solder as replacement for Sn-Pb eutectic solder is strongly desired[1]. Lead-free solders are being studied because of regulations to be implemented under the law banning the use of lead, which will come into force in April 2006 under WEEE (Directive on Waste from Electric and Electronic Equipment)[2]. Sn-Ag, Sn-Bi and Sn-Zn solders are these of typical lead-free solders and Sn-Ag solders are the most widely used as lead-free solders owing to their excellent joint strength and mechanical properties. However, the melting temperatures of Sn-Ag solders are higher than that of Sn-Pb eutectic solder[3]. The melting temperatures of Sn-Ag solders can be effectively lowered by Bi addition. And so the mechanical properties and the joint strength of Sn-Ag-Bi solders have been widely investigated in comparison with Sn-Pb eutectic solder[4),5),6),7),8)]. Hirata et al. reported that the joint strength decreases when more than 5 mass% Bi is added to Sn-Ag solders after annealing[5),6)]. Hereafter in this paper, all compositions are expressed in mass%. In the present paper, Zn addition to Sn-3Ag-5Bi solder was carried out in order to improve the joint strength. The Zn addition is expected to modify the interface structure due to the higher activity of Zn to Cu. We investigated the effect of Zn addition to Sn-3Ag-5Bi solder on the joint strength and the joint interface structure.

2. Experimental procedure

For the investigation of joint strength, Cu sheets were made into lap joint specimens using Sn-3Ag-5Bi- (0, 0.1, 0.5, 1.0, 1.5) Zn solders. The Cu sheets were rinsed with acetone and 10% hydrochloric acid to remove surface oxide. The geometry of specimens and the test method are illustrated schematically in Fig. 1. Pairs of Cu sheets were joined using each solder fragment

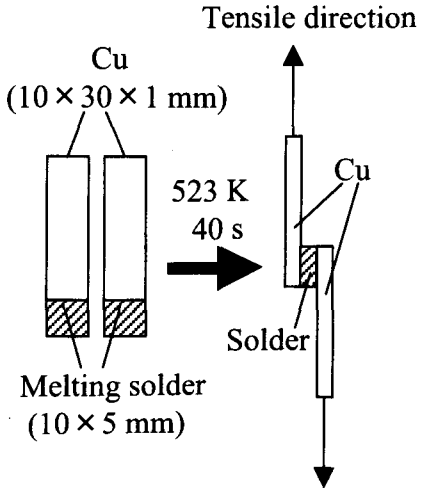

Figure 1 Schematic illustration of joint strength measurement.

(2×2×0.1 mm) by placing them on a hotplate at 523 K for 40 s. The joined specimens were then annealed at 373 K for 3.6 Ms. The joint strength of the as-joined and annealed specimens was measured by an Instron model machine at cross head speed of 0.17 mm/s at 293 K. A crosssection of each specimen was ground by five grades of SiC papers (# 80, 280, 400, 1000 and 1500) and was polished with Al_2O_3 paste (0.3 μm). They were then observed by using a scanning electron microscope (SEM) with energy dispersive X-ray spectroscopy (EDS) and a scanning ion microscope (SIM). The measured value of the reaction layer thickness was expressed as the average of ten thickness measurements in the backscattered electron image. Specimens for transmission electron microscope (TEM) observation were also prepared by using a focused ion beam (FIB). The structures of the reaction layers were observed by TEM and each reaction layer was identified by its electron diffraction pattern.

3. Results and discussions

3.1 Joint strength

The variation in the joint strength of Sn-3Ag-5Bi- (0, 0.1, 0.5, 1.0, 1.5) Zn solders as a function of a square root of annealing time at 373 K is shown in Fig. 2. Standard deviation of the joint strength of Sn-3Ag-5Bi- (0, 0.1, 0.5, 1.0, 1.5) Zn was within 3. The decreasing rates were calculated from the difference of the joint strength of as-joined and after annealing at 373 K for 3.6 Ms are shown in Fig. 3. The joint strength of Sn-3Ag-5Bi- (0, 0.1, 0.5, 1.5) Zn solders almost decreased linearly with increasing annealing time. On the other hand, the joint strength of Sn-3Ag-5Bi-1.0Zn solder did not show any significant decrease after annealing. Thus, Zn addition inhibited decrease in joint strength. The suitable Zn additioncontent was 1.0%. It is the interesting feature that the joint strength linearly decreased with a square root of annealing time. It is considered that this phenomenon relates to diffusion-controlled phenomenon at the joint interface between solder and Cu.

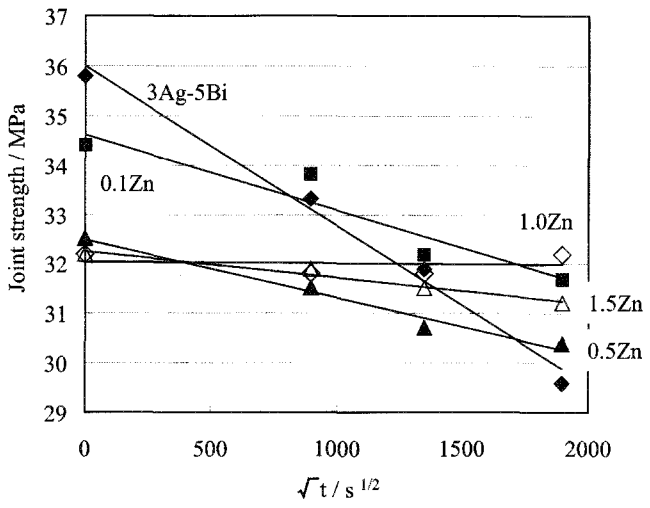

Figure 2 Joint strength of several solders as a function of the square root of annealing time at 373 K.

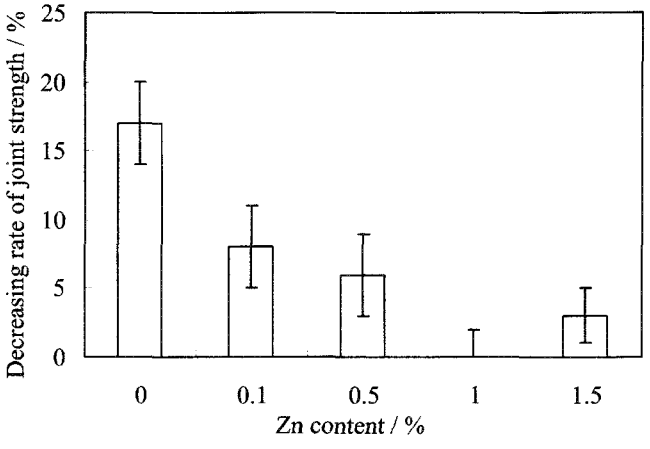

Figure 3 Decreasing rates of joint strength for several solders.

3.2 Joint interface structure

Backscattered electron images of the interfaces of Sn-3Ag-5Bi/Cu and Sn-3Ag-5Bi-1Zn/Cu in the as-joined state and after annealing for 3.6 Ms are shown in Fig. 4. SIM images of the interfaces of Sn-3Ag-5Bi/Cu and Sn-3Ag-5Bi-1Zn/Cu after annealing for 3.6 Ms are shown in Fig. 5. The reaction layers of the interfaces between the solders and Cu grew with increasing annealing time. The interface of Sn-3Ag-5Bi/Cu consists of two reaction layers. These reaction layers were identified by EDS analysis as Cu_6Sn_5 and Cu_3Sn, respectively. The Cu_3Sn, which was located between the Cu_6Sn_5 and Cu, had fine grain size and was clearly observed in the SIM images. The Cu_3Sn layer is very thin and has flat interfaces with the Cu_6Sn_5 layer and with the Cu substrate, while the Cu_6S_5n layer exhibits rough interface. The Cu_6Sn_5 layer markedly grew under annealing, but Cu_3Sn layer grew only slightly. This interface layer structure and the growth phenomenon of the reaction layer were similar to the interfaces of Sn-37Pb, Sn-3.5Ag and Sn-58Bi solder/Cu systems[3),9),10)].

The interface of Sn-3Ag-5Bi-1Zn/Cu also consisted of two reaction layers. These reaction layers were measured as Cu-Sn and Cu-Zn intermetallic compounds by using EDS analysis. As viewed

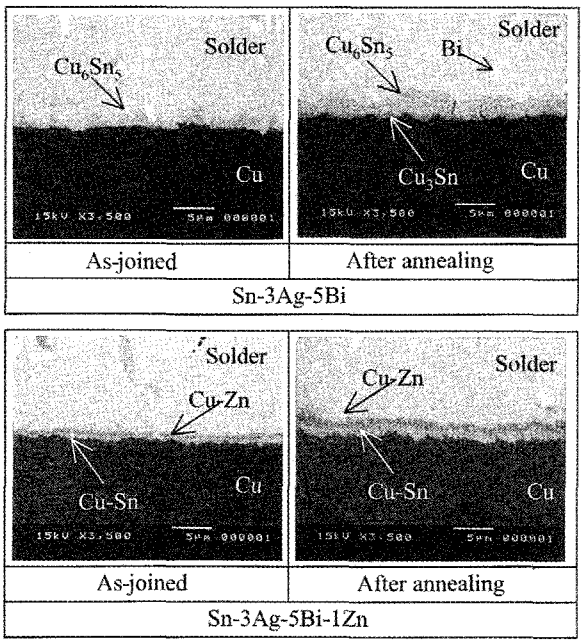

Figure 4 Backscattered electron images of Sn-3Ag-5Bi and Sn-3Ag-5Bi-Zn as-joined and after annealing at 373 K for 3.6 Ms.

in SIM images, the grains of the Cu-Sn and Cu-Zn intermetallic compounds have almost the same size. The Cu-Sn and Cu-Zn intermetallic compounds maintained flat interface after annealing and both reaction layers grew at the same rate. These intermetallic compounds could not be identified by EDS analysis, because they were too thin. Therefore, the reaction layers of Sn-3Ag-5Bi/Cu and Sn-3Ag-5Bi-1Zn/Cu were investigated in detail by using TEM. TEM microstructures and electron diffraction patterns of the reaction layers at Sn-3Ag-5Bi/Cu and Sn-3Ag-5Bi-1Zn/Cu are shown in Fig. 6. The grains measured electron diffraction patterns are indicated by P1, P2, P3 and P4 in Fig. 6. The crystal structure of each reaction layer was determined from its electron diffraction pattern. P1 reaction layer was identified as Cu_3Sn phase of crystal structure A3. P2 reaction layer was identified as Cu_6Sn_5 phase of crystal structure $B8_1$. P3 was identified as Cu_6Sn_5 phase of crystal structure $B8_1$ and P4 was identified as Cu_5Zn_8 phase of crystal structure $D8_2$. Addition of 1% Zn changed the interface structure from solder/Cu_6Sn_5/Cu_3Sn/Cu to solder/Cu_5Zn_8/Cu_6Sn_5/Cu.

The reaction layer thicknesses of several solders as a function of a square root of annealing time at 373 K are shown in Fig. 7. The standard deviations of reaction layer thicknesses at each annealing time are shown in Table 1. The reaction layers of all solders increased linearly with a square root of annealing time. This suggests that this reaction at the interfaces of these solders/Cu is diffusion-controlled. Slopes, y intercepts and correlation coefficients of each line by the least-squares method are shown in Table 2. Zn addition caused the thickness of the reaction layer to become thin as-joined and after annealing. Further, the slope for Sn-3Ag-5Bi-1Zn solder became the smallest among the all Zn addition solders. The growth of the reaction layer at Sn-3Ag-5Bi/Cu was dominated by the Cu_6Sn_5 layer that grew markedly into the solder. On the other hand, in the case of Sn-3Ag-5Bi-1Zn solder, it is suggested that the Cu_5Zn_8 layer acts as a diffusion barrier that inhibits the growth of the Cu_6Sn_5 layer with annealing. The suitable Zn additioncontent is 1 % from the viewpoint of inhibiting decrease the joint strength and the growth of a Cu_6Sn_5 layer.

Backscattered electron images of Sn-3Ag-5Bi-1.5Zn/Cu as-joined and after annealing are shown in Fig. 8. The as-joined interface consisted of the layers of Cu_6Sn_5 and Cu_5Zn_8. But after annealing, a part of Cu_5Zn_8 broken down and Cu_6Sn_5 grew into solder. Excess Zn occurring in a solder added with more than 1.5% Zn diffused to the Cu side where it formed Cu_5Zn_8. So the joint strength at 1.5% Zn addition decreased about 3 %. It was suggested that the maintenance of the joint strength was due to the interface structure that maintained the layer interface of solder/Cu_5Zn_8/Cu_6Sn_5/Cu after annealing.

Table 1 Standard deviation of reaction layer thicknesses at each annealing time.

Zn content / %	0h	225h	506h	1000h
0.0	0.3	0.3	0.5	0.5
0.1	0.2	0.4	0.5	0.5
0.5	0.3	0.3	0.4	0.5
1.0	0.2	0.4	0.3	0.4
1.5	0.3	0.4	0.4	0.5

Table 2 Slopes, y intercepts and correlation coeffients of lines by a least-aquares method.

Zn content/%	Slope	y intercept	R
0.0	0.020	2.254	0.96
0.1	0.026	1.499	0.93
0.5	0.022	1.448	0.98
1.0	0.015	1.093	0.91
1.5	0.028	0.904	0.91

3.3 Microstructure of joint interface

Backscattered electron images of crosssections of fractures for Sn-3Ag-5Bi and Sn-3Ag-5Bi-1Zn after annealing are shown in Fig. 9. The white precipitations observed in the solder and at the joint interface are Bi grains. Bi grains of Sn-3Ag-5Bi solder were observed more than those of Sn-3Ag-5Bi-1Zn solder. It is thought that Bi grains in the solder precipitated by annealing for the excess

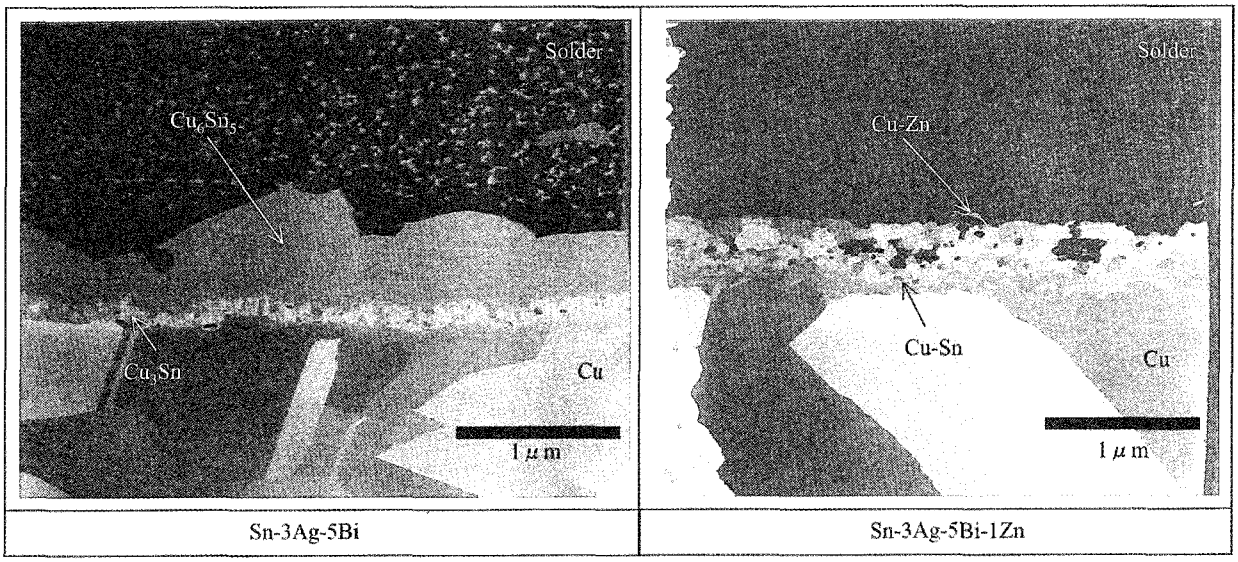

Figure 5 SIM images of Sn-3Ag-5Bi and Sn-3Ag-5Bi-Zn after annealing.

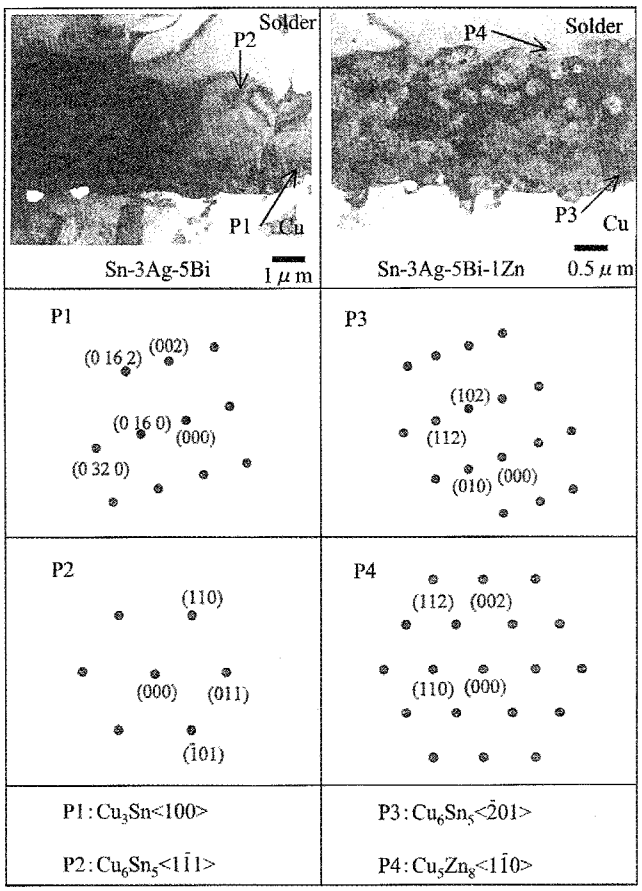

Figure 6 TEM microstructures and electron diffraction patterns of Sn-3Ag-5Bi and Sn-3Ag-5Bi-Zn.

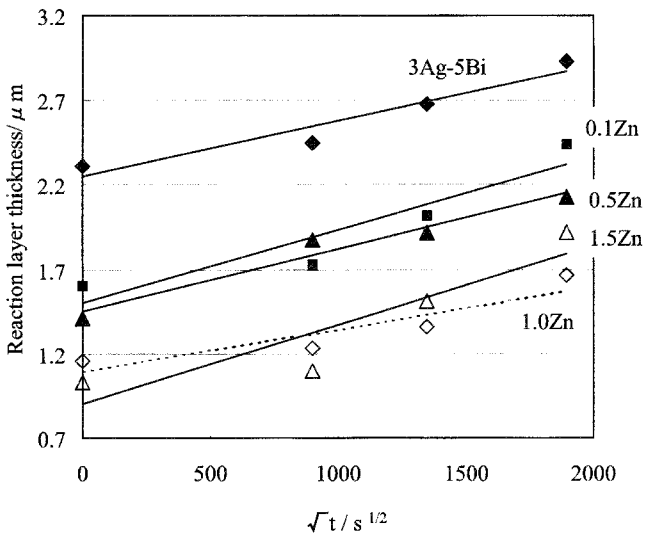

Figure 7 Reaction layer thickness of several solders as a function of the square root of annealing time at 373 K.

solid solubility of Bi to Sn. Cu_6Sn_5 was formed and grew at the interface with annealing. As result, the Bi content in the solder increased around Cu_6Sn_5, and Bi grains precipitated at the interface around Cu_6Sn_5. The amount of precipitation Bi grain at the joint interface is related to the growth of Cu_6Sn_5, so the amount of Bi grain at the joint interface is greater for Sn-3Ag-5Bi solder than for Sn-3Ag-5Bi-1Zn solder because of larger growth of Cu_6Sn_5.

The crack propagation of Sn-3Ag-5Bi solder at the joint interface is shown in Fig. 10. The crack propagation in the as-joined state was observed between Cu_3Sn and Cu. On the other hand, the crack propagation after annealing was observed between Cu_6Sn_5 and solder. The reason is that brittle Bi grains precipitated between Cu_6Sn_5 and solder owing to the annealing by the mechanism described above. Therefore, the crack propagation site changed. So the precipitation of Bi grain between Cu_6Sn_5 and solder caused by annealing decreases the joint strength of Sn-3Ag-5Bi solder. On the other hand, the crack propagations of Sn-3Ag-5Bi-1Zn solder in the as-joined and annealed states were observed

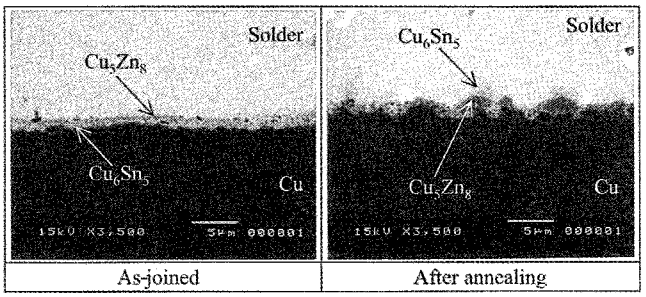

Figure 8 Backscattered electron images of Sn-3Ag-5Bi-1.5Zn as joined and after annealing at 373 K for 3.6 Ms.

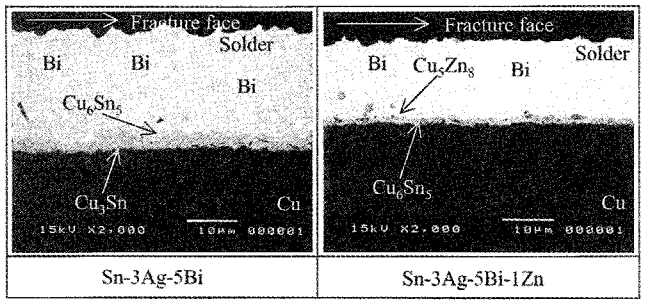

Figure 9 Backscattered electron images of crosssections of fractures for Sn-3Ag-5Bi and Sn-3Ag-5Bi-1Zn after annealing.

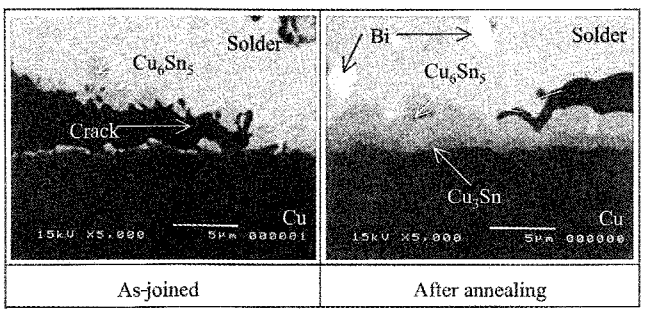

Figure 10 Backscattered electron images of crack propagations for Sn-3Ag-5Bi as-joined and after annealing.

between Cu_5Zn_8 and solder as shown in Fig. 9. Therefore, the joint strength of Sn-3Ag-5Bi-1Zn solder did not change after annealing.

4. Conclusions

The effect of Zn addition to Sn-3Ag-5Bi solder on the joint strength and the joint interface structure were investigated. The main results obtained were as follows :

(1) The joint interface structure changed from solder/Cu_6Sn_5/Cu_3Sn/Cu to solder/Cu_5Zn_8/Cu_6Sn_5/Cu by Zn addition.

(2) The decrease in the joint strength and the growth of reaction layer after annealing at 373 K for 3.6 Ms are inhibited by Zn addition.

(3) Cu_5Zn_8 layer formed by Zn addition acted were a barrier layer for the growth of Cu_6Sn_5.

(4) Optimum Zn additioncontent to Sn-3Ag-5Bi solder was 1 % from viewpoint of the joint strength and the joint interface structure.

REFERENCES

1) J. Glazer : "Metallurgy of low temperature Pb-free solders for electronic assembly," International Materials Reviews, 40, pp.65-93 (1995).

2) WEEE (Directive on Waste from Electric and Electronic Equipment) (2000).

3) Y. Nakahara, J. Matsunaga and R. Ninomiya : Proc. 6th Sympo. on Microjoining and Assembly Technologies for Electronics, 1999, Yokohama Japan, pp.341-46 (in Japanese).

4) T. Takemoto, M. Takahashi, A. Matsunawa, R. Ninomiya and H. Tai, Quarterly Journal of the Japan Welding Society, 16, pp.87-92 (1998).

5) Y. Hirata, Y. Kariya and M. Otsuka, Proc. 5th Symposium on Microjoining and Assembly Technology in Electronics, 1999, Yokohama Japan, pp.421-6 (in Japanese).

6) I. Mori, S. Fujiuchi, A. Hirose, K. Fujimoto and T. Takemoto, Proc. 6th Symposium on Microjoining and Assembly Technology in Electronics, 2000, Yokohama Japan, pp.355-60 (in Japanese).

7) J. S. Hwang, International Journal of Powder Metallurgy, 37, pp.61-75 (2001).

8) A. Hirose, T. Fujii, T. Imamura and K. Kobayashi, Materials Transaction, 42, pp.794-802 (2001).

9) K. Suganuma and Y. Nakamura, Journal of Japan Institute Metals, 59, pp.1299-305 (1995).

10) K. Suganuma, K. Niihara, T. Moritho and Y. Nakamura, Journal of Japan Institute of Electronics Packaging, 12, pp.406-12 (1997).